Available online at www.sciencedirect.com
SCIENCE DIRECT®

Polymer 45 (2004) 3457–3463

polymer

www.elsevier.com/locate/polymer

Dynamic mechanical properties of annealed sulfonated poly(styrene-*b*-[ethylene/butylene]-*b*-styrene) block copolymers

R.I. Blackwell, K.A. Mauritz*

Department of Polymer Science, The University of Southern Mississippi, Hattiesburg, MS 39406-0076, USA

Received 26 August 2003; received in revised form 2 February 2004; accepted 3 February 2004

Abstract

Solution cast films of lightly sulfonated styrene-*b*-[ethylene-*co*-butylene]-*b*-styrene, (sSEBS) block copolymers were annealed for various times at 120 °C and thermal transitions are evaluated using dynamic mechanical analysis. Increased annealing time and increase in degree of sulfonation increases T_g for the PS phase while T_g for the EB phase is practically unchanged, and in some cases, there is suggestion of a relaxation due to EB–PS inter-phases. Annealing has a minor effect on the rubbery plateau storage modulus. Thus, annealing primarily alters the PS block phase. EB–PS phase separation appears to be refined with increasing SO_3H content. The region of rubber elasticity extends to higher temperatures with increased degree of sulfonation. A high temperature dynamic mechanical transition that is tentatively attributed to disruption of SO_3H—rich sub-domains within the PS block domains shifts to higher temperature with annealing.

Keywords: Block copolymer; Sulfonation; Annealing

---

1. Introduction

Mauritz and coworkers have employed lightly sulfonated poly(styrene-*co*-isobutylene-*co*-styrene) block copolymers (BCPs) [1,2] as well as poly[styrene-*co*-(ethylene/butylene)-*co*-styrene] (SEBS) [3–5] BCPs as morphological templates, in the sense of domain-targeted sol–gel reactions of hydrolyzed metal alkoxides, in an effort to create novel organic–inorganic nanocomposite materials. These two similar BCPs have nanophase-separated morphologies consisting of PS blocks segregated into ordered sphere, hexagonally packed rod, or lamellar geometries as the styrene volume fraction (f_{PS}) increases. This is the same morphological progression as exists for the simpler PS-polydiene di-block copolymers for which there is also an ordered bicontinuous double diamond morphology reported for f_{PS} in the range 0.28–0.34 [6]. These di-block copolymers, however, do not possess the mechanical integrity of the tri-block copolymers owing to PS blocks in the latter that are situated at both ends of the chain and aggregate to form thermally reversible crosslinks. The tri-block materials are useful thermoplastic elastomers for $f_{PS} < 0.5$. For $f_{PS} > 0.5$, there is hard–soft block phase inversion and these tri-block copolymers act as rubber-toughened plastics.

The cohesiveness of the PS block domains, and subsequent mechanical strength, modulus and solvent resistance can be increased by sulfonating these blocks which serves to enhance inter-block interactions through hydrogen bonding. Also, the SO_3H groups can be ion exchanged to various cation forms [7] to adjust electrostatic interactions to a degree depending on counterion size and valence, and whether the counterion is of a mineral or organic nature. It is of particular interest in this research to adjust the energetic environment within the PS blocks so that these domains are highly compatible with hydrolyzed inorganic alkoxides that have, for example, polar SiOH groups. In this way, domain-targeted sol–gel reactions can occur and this process forms the basis of our *template hypothesis* in the effort to create organic/inorganic nanocomposite materials wherein an intimately incorporated inorganic oxide phase is constructed molecule-by-molecule. This process stands in contrast with the formation of polymer/clay(aluminasilicate) nanocomposites wherein preformed particles are mixed into the polymer by physical means and there are fundamental concerns of whether the particles are exfoliated and well-dispersed.

---

* Corresponding author. Tel.: +1-601-266-5595; fax: +1-601-266-5635.
E-mail address: kenneth.mauritz@usm.edu (K.A. Mauritz).

0032-3861/$ - see front matter © 2004 Elsevier Ltd. All rights reserved.
doi:10.1016/j.polymer.2004.02.010

If sulfonated block copolymers are to be used as sol–gel reaction templates, the following questions must be addressed. (1) Will sulfonation, which increases the effective PS block volume fraction and inserts strong interactions, result in a morphological shift, and (2) are the morphologies of an equilibration nature? The first concern has been addressed in an earlier report in which it was disclosed that SEBS sulfonation causes a morphological shift from hexagonal-packed rods to a lamellar structure [8]. On the other hand, sulfonation of the poly(styrene-co-isobutylene-co-styrene) materials does not cause a morphological shift [1], but subsequent conversion of the acid groups to $Na^+SO_3^-$ groups induces a frustrated morphology with considerably less order [2]. The second concern arises from the fact that strong inter-block interactions can slow the kinetics of the evolution of equilibrium morphologies. It is for this reason that the annealing experiments reported here were conducted.

Fig. 1 consists of TEM micrographs for the following unannealed samples: unmodified SEBS illustrating the well-developed, expected morphology of hexagonal-packed PS cylinders that are (a) normal and (b) parallel to the plane of the image, (c) an 8% H^+ sSEBS sample showing a less ordered morphology, and (d) a 14% H^+ sSEBS sample showing lamellar morphology [8]. Micrographs (a), (b) and (d) clearly show ordered structures and (c), shows phase separation, but with less order, which has been described as a frustrated morphology. Sample (c) had the same thermal-drying history as the other two and the frustrated morphology is considered to be a transitional condition over the range of sulfonation.

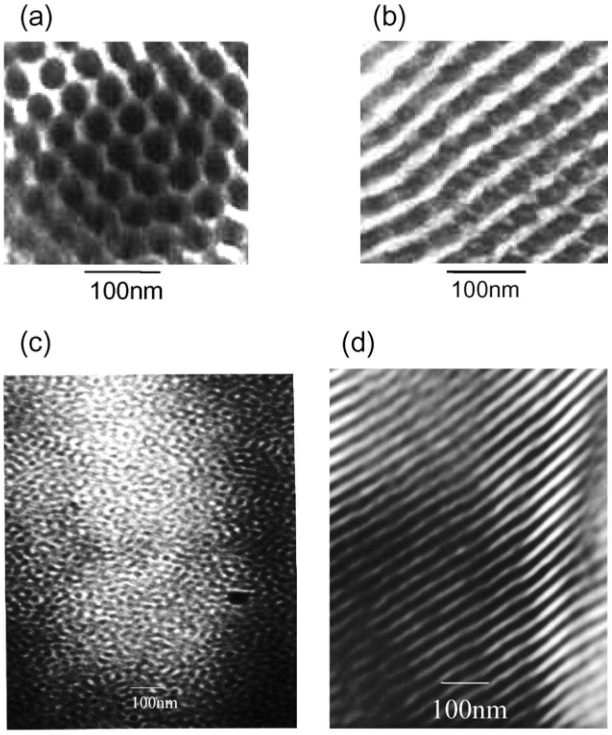

Fig. 1. TEM images of unmodified SEBS illustrating HPC morphology of PS cylinders that are (a) normal and (b) parallel to the plane of the image. (c) TEM image of an 8% H^+ sSEBS sample showing a frustrated morphology. (d) TEM images of a 14% H^+ sSEBS sample showing lamellar morphology.

The glass transition of the PS block phase increases with sulfonation but it is also important to know whether the glass transition of the EB inner block and rubbery plateau modulus is influenced in this way. Reported here is the effect of time and temperature of annealing on the dynamic mechanical behavior of a lightly sulfonated SEBS copolymer. Annealing, in principle, is expected to refine the phase-separated morphology of samples that have not achieved equilibrium and reduce S/EB interphase regions. Annealing might also be thought of as minimizing the electrostatic energy in the PS block domains while maximizing the entropy of the EB blocks in non-equilibrium samples.

2. Experimental

2.1. Materials

All reagents were used without further purification. 1,2-dichloroethane (DCE) (99.8%), toluene, 1-hexanol (98%), acetic anhydride (ACS grade), and sulfuric acid (ACS grade) were obtained from Fisher Co. The SEBS copolymer, Kraton® G1652, which is hydrogenated styrene/butadiene/styrene, was obtained from Kraton® LLC and had $M_n \approx 50,000$ g/mol, as determined by GPC, and a styrene content of ~30 mol%, as determined by ^1H NMR.

2.2. Sulfonation

Sulfonation of the block copolymer was carried out according to the procedure of Weiss et al. [9] In summary, the BCP was dissolved in DCE at 50 °C. The sulfonating agent, acetyl sulfate, was generated by addition of sulfuric acid to a solution of acetic anhydride in DCE. The desired amount of acetyl sulfate as necessitated by the desired level of sulfonation was added to the polymer solution. The reaction proceeded for 2 h and the polymer was recovered by steam stripping. Mole percent sulfonation was determined by dissolving sSEBS samples in a toluene/hexanol mixture and titrating against a standardized base to a phenolphthalein endpoint. This method determines sulfonation levels consistently within 2–3% of what is found by elemental analysis.

2.3. Film casting

A 10% solution of the parent BCP in toluene was cast in a PTFE dish and allowed to dry at 60 °C under N_2 for 5 days. The film was then annealed in a vacuum oven (30 inHg) at 120 °C for various times. Film casting of the sulfonated BCP was accomplished in the same manner with the exception that hexanol was added as a co-solvent.

2.4. Dynamic mechanical analyses

Dynamic mechanical analysis (DMA) was performed using a Seiko Instruments SDM5600 Viscoelasticity Analysis System with DMS 210 Tension Module. Samples were tested at a frequency of 1 Hz at temperatures from −120 to 350 °C at a heating rate of 2 °C/min.

3. Results and discussion

Dynamic mechanical storage modulus, E', and lost tangent, tan $\delta = E''/E'$ ($E' =$ loss modulus) vs. temperature (T) curves for the parent BCP (PBCP) at various annealing times are shown in Fig. 2a and b, respectively. The rubbery plateau modulus is relatively unaffected by annealing time, and actually decreases slightly after annealing for 24 h. This implies that the casting/drying conditions were sufficient for the development of equilibrium morphology. The unchanging widths of the tan δ peaks corresponding to the glass transition of both the ethylene/butylene (EB) and PS phases also suggests that annealing at elevated temperatures does not affect interphase regions, i.e., phase structure refinement, in the PBCP. The TEM images in Fig. 1 show distinct phase separation in pre-annealed samples and annealing is not expected to cause considerable further refinement. With regard to the small drop in the rubbery plateau after 24 h, the situation is unclear as this behavior is usually diagnostic of lowered effective crosslinking in elastomers, and the PS blocks are the effective crosslinks in these thermoplastic systems. It might be considered that the rubbery modulus of the un-annealed sample is highest because of partial mixing of PS into the interfaces and/or EB blocks in a condition of unrefined phase separation. However, distinct phase separation does exist before annealing as seen in the TEM micrographs, and, moreover, the relaxation peak widths are essentially unchanged with annealing and the tan δ curves in the rubbery temperature regime, i.e., between the two glass transition peaks, are essentially the same.

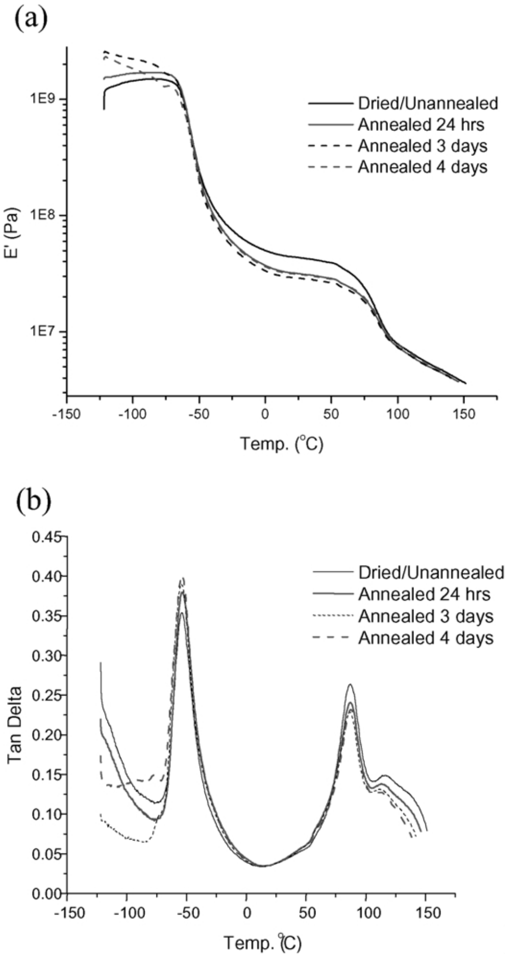

Fig. 2. E' and tan δ vs. T curves for the parent BCP annealed at 120 °C for various times.

Table 1 summarizes transition temperatures, defined in terms of the peak maxima seen in Fig. 2b, at each annealing time for the EB phase glass transition, PS phase glass transition, and a high temperature transition (HTT). This HTT has been attributed in the literature to a lattice-disordering temperature which precedes the order–disorder transition (ODT) [10], although the ODT for this material has been reported at the considerably higher temperature of ~230 °C based on SAXS analysis [11]. Our results actually showed an *order–order* transition (OOT) at ~240 °C and an ODT for this BCP is not detected below the temperature at which the material degrades [8]. In any case, it is unlikely that a lattice-disordering transition would occur above 100 °C and below the ODT or OOT. It is difficult to speculate on the nature of this transition because it occurs as the sample begins to flow. However, as discussed later, this transition in the parent BCP may not be the HTT found in the sulfonated SEBS material.

The transitions observed on the tan δ vs. T plots remain constant for annealing times at least as great as 4 d. The majority of toluene solvent (boiling point ~111 °C) is removed from the samples during the casting/drying procedure. If a significant amount of toluene were still present in un-annealed films, the transitions would be shifted to a lower temperature due to plasticization. The consistency in transition temperatures and general curve shapes further suggests that this annealing procedure does not influence PS/EB interphases or domain geometry in the PBCP.

Fig. 3a and b are the E' and tan δ vs. T curves for a 4% sulfonated BCP sample. Hereafter, percent sulfonation will

Table 1
Thermal transitions for the unmodified parent block copolymer

Annealing time	EB T_g (°C)	PS T_g (°C)	HTT (°C)
Un-annealed	−54	87	117
24 h	−53	88	114
3 d	−53	88	114
4 d	−53	89	114

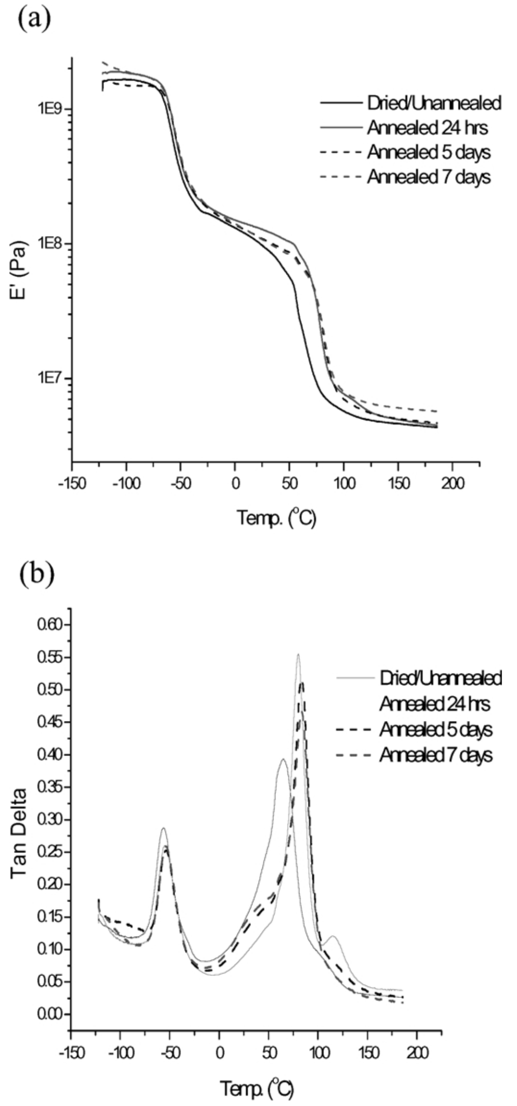

Fig. 3. (a) E' and (b) tan δ vs. T curves for a 4% H^+ sSEBS sample that was annealed at 120 °C for various times.

be indicated by X%H^+ sSEBS; in this case X = 4. The rubbery plateau is elevated somewhat by annealing and the largest change in E' occurred after 1 d. Hexanol was used as the co-solvent in the sulfonated samples with a view toward disruption of hydrogen bonding between SO_3H groups on different PS blocks. However, hexanol (boiling point ~156 °C) is more difficult to remove as compared to toluene due to hydrogen bonding interactions between the hexanol OH and SO_3H groups. Perhaps the drying conditions are insufficient for complete hexanol removal, but annealing for 24 h removes the remaining hexanol so that the slight increase in modulus might be accounted for in terms of increased interactions between sulfonic acid groups. In thermoplastic elastomers of this type, the hard blocks are viewed as a form of crosslink and the increase in T_g (sPS) is interpreted in terms of interactions between inserted sulfonate groups that render the PS domains more cohesive and thereby impart a higher modulus.

This interpretation is commensurate with the behavior of the tan δ vs. T plots. Annealing of the parent BCP has little effect on the thermal transitions, which indicates that the unmodified sample possessed equilibrium morphology under these processing conditions. However, annealing does significantly influence the PS phase T_g and HTT of the 4%H^+ sSEBS sample. The transition temperatures for the annealed sSEBS samples are listed in Table 2. The PS phase T_g increases by a significant 15 °C after 24 h of annealing and the associated tan δ peak becomes much narrower. This peak narrowing might reflect a narrowing of the PS/EB interphase thickness, and therefore phase separated morphology refinement. However, the EB phase T_g remains constant, which supports the aforementioned view that residual hexanol molecules remain in the sulfonated PS regions after drying and prior to annealing. Beyond 1 d annealing, the PS phase T_g increases only slightly and the tan δ peaks have a low temperature shoulder that is weakest for the 1 d-annealed sample. There is a HTT in the form of a shoulder on the tan δ curve for the un-annealed sample. The weakness of this transition may be due to the broadness of the PS phase T_g caused by hexanol plasticization of the PS domains that would broaden the distribution of relaxation times. After 24 h annealing, there is a very distinct high temperature peak. There is also a HTT after 5 d annealing, although not as distinct. This might indicate that the HTT in the 4% H^+ sSEBS material is not of the same nature as that in the parent BCP.

Based on the studies of Weiss et al., it might be considered that the third, HTT in the sSEBS materials is due to the formation of SO_3H— rich sub-domains in the PS block domains when the degree of sulfonation is sufficiently high. The materials in this work do not have $SO_3^-Na^+$ ion pairs in the PS blocks as in the materials of Weiss et al. However, there can be proton dissociation in low pK_a sulfonic acid groups in the presence of residual water that give rise to strong electrostatic interactions between $-SO_3^-H_3^+O$ charged moeities during film formation. After sample drying, PS chain segments in the vicinity of associated acid groups, between which there are strong electrostatic, or at least hydrogen bonding interactions, will have restricted mobility in a manner similar to that as described by Eisenberg et al. in their multiplet-cluster model for ionomers [12]. Although the qualitative model of Eisenberg et al. was based on random ionomers, the general concept of having extended regions of restricted chain mobility around SO_3H group aggregates within the PS block

Table 2
Thermal transitions for 4% H^+ sSEBS

Annealing time	EB T_g (°C)	PS T_g (°C)	HTT (°C)
Dried/un-annealed	−56	65	N/A
24 h	−55	80	116
5 d	−54	83	N/A
7 d	−54	83	N/A

domains is reasonable with appropriate allowance being made for the morphological constraints in this phase separated system. T_g for this PS block sub-phase would be greater than that for an unsulfonated PS block phase, or unsulfonated regions within a sulfonated block phase, and would increase with increasing degree of sulfonation. Strong $-SO_3H$ associations in these aggregates would be disrupted upon annealing at sufficiently high temperatures. These concepts are in the realm of speculation and are offered as possible mechanisms for consideration.

At 4% sulfonation, the regions of restricted mobility are viewed as being large enough to result in a third T_g and, ultimately, the SO_3H-poor and SO_3H-rich phases are miscible above some temperature that increases with increasing percent sulfonation. At 4% sulfonation, annealing at 120 °C for 5 d is apparently sufficient to achieve miscibility throughout the PS domains as seen by a suppression of the HTT. There is a slight increase in the PS block T_g resulting from an increase in sulfonic acid content, as is observed in Fig. 3b. There is also a low temperature shoulder on the PS block glass transition peak that becomes significant after 5 d of annealing. This shoulder was not seen for the parent block copolymer, which, however, was only annealed for 4 d. Perhaps this shoulder is the fingerprint of unique interphases that develop with annealing in this particular case. Theoretically, an endothermic sPS/EB block mixing interaction parameter, χ_{EB-PS}, would decrease with increasing temperature which would have the effect of increasing interphase thickness. Of course, the usual assumption of weak interactions being operative in endothermic systems is not quite valid because strong SO_3H–SO_3H interactions within the PS block present a barrier to phase miscibility. For one, the kinetics of thermally stimulated macromolecular reorganization would be considerably slower and it would be more difficult for sections of PS blocks to cross the interfaces in a thermodynamic drive toward mixing.

The same trends hold true for the 7% H^+ sSEBS sample, as seen in Fig. 4a and b, but with notable differences (Table 3). Compared with the 4% H^+ case, the HTT is somewhat more distinct for the un-annealed sample. Both the PS block T_g and the HTT for 24 h are shifted to higher temperatures compared with the same annealing temperatures for 4% sulfonation. This is significant considering that the increase in sulfonation is only 3%. If this small increase in sulfonation is distributed over the entire lengths of the PS block, it might be thought that all transitions associated with the hard domains would be affected. Similar to the case of 4% sulfonation, the HTT is no longer observed after 5 d annealing and the PS T_g increases up to 7 d. The low temperature shoulder on the PS transition again becomes apparent after 5 d annealing and the same comments regarding interphases are offered.

Table 3
Thermal transitions for 7% H^+ sSEBS

Annealing time	EB T_g (°C)	PS T_g (°C)	HTT (°C)
Dried/un-annealed	−57	56	90
24 h	−55	87	129
5 d	−54	92	–
7 d	−54	93	–

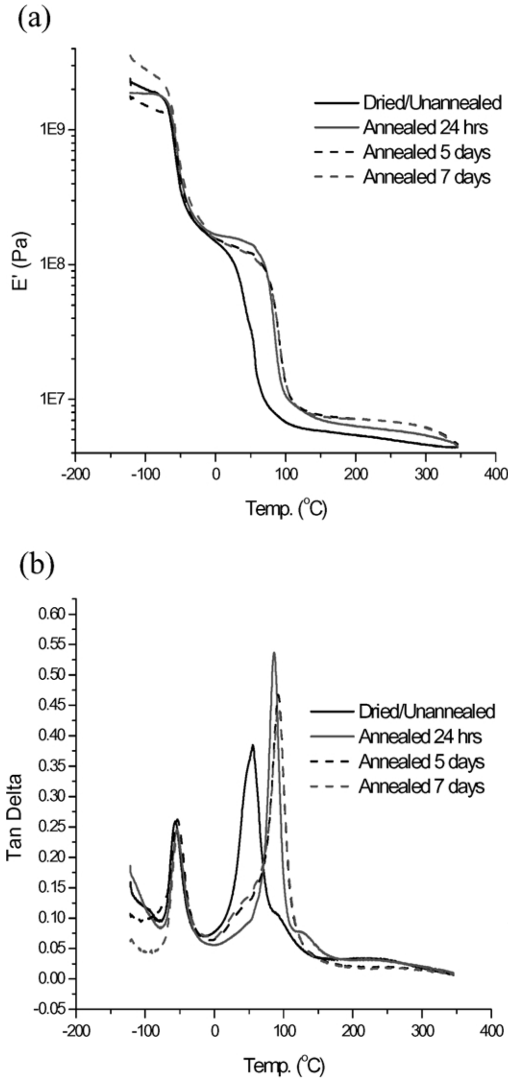

Fig. 4. (a) E' and (b) tan δ vs. T curves for 7% H^+ sSEBS annealed at 120 °C for various times.

Although the EB phase T_g is essentially invariant, it drops slightly with increased annealing time; this is also seen for the case of 4% sulfonation in Table 2. As for the 4% sulfonated sample, moduli along the rubbery plateau for 7% sulfonation are increased and the region of rubber elasticity is extended to higher temperatures with annealing. However, the temperature range over which the material is rubbery is considerably narrower for 7% H^+ sSEBS.

The E' and tan δ vs. T curves for a 12% H^+ sSEBS sample are shown in Fig. 5a and b (Table 4). Again, the same general trends hold true with a few exceptions. Both the PS block phase glass transition and the HTT tan δ peaks are sharper for the annealed samples, which can be

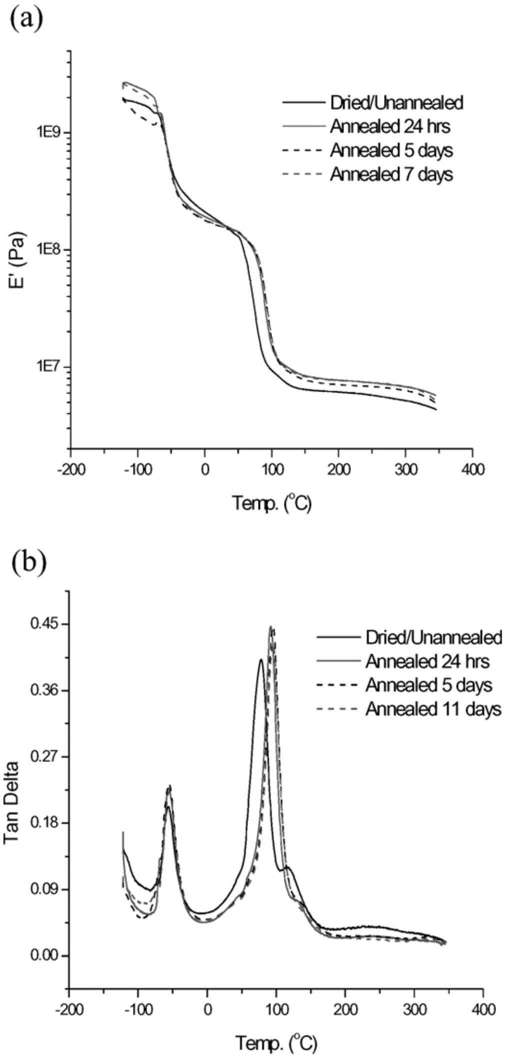

Fig. 5. (a) E' and (b) tan δ vs. T curves for 12% H^+ sSEBS annealed at 120 °C for various times.

rationalized in terms of refinement of EB–PS phase separation morphology. In this view, χ_{EB-PS} would increase with increasing sulfonic acid content. The PS block T_g increases significantly, by around 15 °C, with sulfonation to this degree. The curves for all annealing times are rather superimposed and the PS block T_g remains constant. The rubbery plateau sections are also essentially the same while the region of elasticity is pushed to higher temperatures. However, the HTT temperature increases with annealing time, and is higher than that for the same time for 7% sulfonation. If the HTT is in fact associated with the disruption of SO_3H clusters within the PS block regions, it might be concluded that, at 12% sulfonation, these clusters are stabilized by hydrogen bonds to an extent that they can withstand time-temperature annealing conditions up to at least 5 d. After 11 d, however, the HTT is no longer observed. It is also noted that, as opposed to the situation for samples having lower degrees of sulfonation, the low temperature shoulder on the PS block transition is absent for the 12% sample, even after 11 d annealing. The increase in sulfonation would increase χ_{EB-PS}, thereby diminishing phase miscibility and causing mixed interphase regions to diminish.

The E' and tan δ vs. T curves for a 17% sulfonated sample are seen in Fig. 6a and b. While the region of rubber elasticity has again been extended to higher temperatures, all of the E' curves are essentially superimposed in this temperature range. Evidently, the effect of SO_3H interactions has attained a state of saturation with regard to their influence on the rubbery modulus. The PS block T_g has been considerably elevated and then slightly increases with increasing annealing time, as seen in Table 5. There is no

Table 4
Thermal transitions for 12% H^+ sSEBS

Annealing time	EB T_g (°C)	PS T_g (°C)	HTT (°C)
Dried/un-annealed	−56	79	118
24 h	−56	94	135
5 d	−53	96	146
11 d	−53	94	–

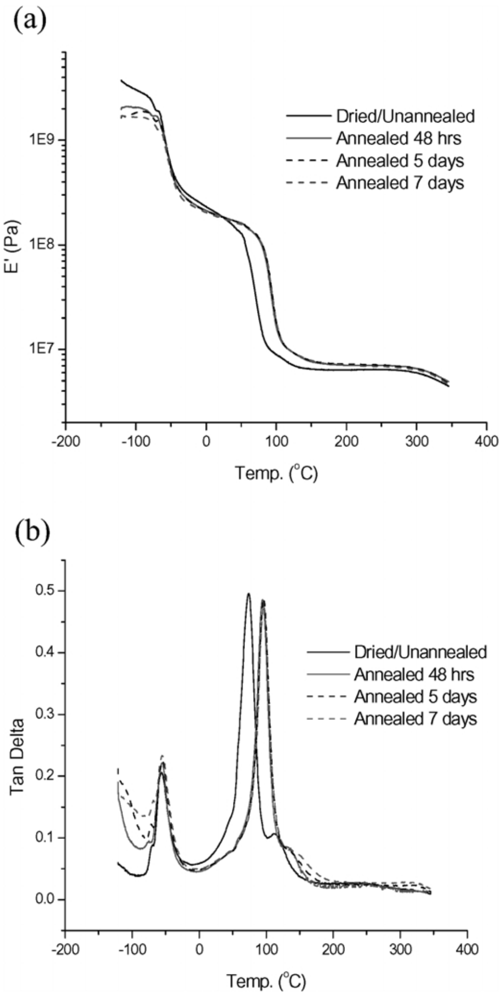

Fig. 6. (a) E' and (b) tan δ vs. T curves for 17% H^+ sSEBS annealed at 120 °C for various times.

Table 5
Thermal transitions for 17% H^+ sSEBS

Annealing time	EB T_g (°C)	PS T_g (°C)	HTT (°C)
Dried/un-annealed	−56	72	114
48 h	−55	95	138
5 d	−56	96	142
7 d	−54	97	149

suggestion of mixed interface owing to the absence of a low temperature shoulder on the tan δ curve, as seen for the lower-sulfonated samples, for the PS block phase glass transition. The EB phase T_g remains basically the same vs. annealing time and is the same as that for the un-annealed sample, which suggests that annealing does not affect chain mobility in the rubbery phase.

However, the HTT temperature monotonically increases by 24 °C with the first annealing, and, thereafter, up to 7 d of annealing, has a net increase of 35 °C. Again, the view that is offered is that annealing induces strong cohesion in the PS sub-domain regions consisting of SO_3H aggregates. Samples that have been annealed for longer times would require more thermal kinetic energy i.e., greater temperatures, to disrupt these aggregates, which accounts for the observed behavior.

Viewing the totality of the data over the range of percent sulfonation and annealing time, it might be suggested that there is a threshold of sulfonic acid content above which clusters of these groups can strongly influence the dynamic mechanical properties. Below this threshold, smaller SO_3H group associations may exist, but the enthalpic penalty associated with disruption of these aggregates and the regions of restricted PS chain mobility in their vicinity is less. Such clusters might be thought of as a kinetically preferred morphology within the time scale of sample preparation, but not an equilibrium morphology, as indicated by the broadening of the HTT at longer annealing times, even for the higher sulfonated samples.

4. Conclusions

Annealing at 120 °C for various times can significantly influence the PS block phase glass transition in sulfonated SEBS block copolymers as well as a higher temperature dynamic mechanical transition that is tentatively attributed to the disruption of SO_3H-rich sub-domains within the PS block domains. Increased annealing and increase in degree of sulfonation increases T_g for the PS phase while T_g for the EB phase is practically unchanged. In some cases, there is the suggestion of a relaxation due to EB–PS inter-phases in the way of a low temperature shoulder on the PS glass transition peaks of tan δ vs. T curves. Annealing has a minor effect on the dynamic rubbery plateau storage modulus and the EB block phase glass transition is not profoundly affected. Thus, annealing primarily alters the PS block phase. EB–PS phase separation is refined with increasing SO_3H content because the tan δ vs. T peak for the PS phase narrows. In cases where there is an absence of a low temperature shoulder on the PS block glass transition and increase in T_g (PS block), it is thought that sulfonation increases χ_{EB-PS}, thereby diminishing phase miscibility and reducing the fraction of mixed interphase regions. The region of rubber elasticity is extended to higher temperatures with increased degree of sulfonation. The same general trends exist for all degrees of sulfonation.

In the future, TEM and AFM studies of these materials will be performed to provide direct visualizations of morphological shifts with annealing.

Acknowledgements

The authors gratefully acknowledge the US Army Research Office (DAAD19-01-0498) for their financial support and Kraton LLC for the donation of the Kraton® G1652 material used in these studies.

References

[1] Mauritz KA, Storey RF, Mountz DA, Reuschle DA. Polymer 2002;43:4315.

[2] Mauritz KA, Storey RF, Reuschle DA, Beck Tan N. Polymer 2002;43:5949.

[3] Blackwell RI, Mauritz KA. Am. Chem. Soc. Div., Polym. Chem. Prepr. 2003;44(1):1128.

[4] Blackwell RI, Mauritz KA. Am. Chem. Soc. Div., Polym. Chem. Prepr. 2003;44(1):1132.

[5] Blackwell RI, Mauritz K. Am. Chem. Soc. Div., Polym. Chem. Prepr. 2002;43(2):1341.

[6] Bates FS, Fredrickson GH. Ann. Rev. Phys. Chem. 1990;41:525.

[7] Weiss RA, Sen A, Willis CA, Pottick LA. Polymer 1991;32:2785.

[8] Blackwell RI, Mauritz KA. Polymer 2004; in press.

[9] Weiss RA, Sen A, Willis CA, Pottick LA. Polymer 1991;32:1867.

[10] Tse MF. J. Adhesion Sci. Technol. 1989;3(7):551.

[11] Lu X, Steckle Jr. WP, Hsiao B, Weiss RA. Macromolecules 1995;28:2831.

[12] Eisenberg A, Hird B, Moore RB. Macromolecules 1990;23:4098.